

## “Snowplow” injection front effects

T. E. Moore,<sup>1</sup> M. O. Chandler,<sup>2</sup> N. Buzulukova,<sup>1,3</sup> G. A. Collinson,<sup>1</sup> E. L. Kepko,<sup>1</sup>  
K. S. Garcia-Sage,<sup>1</sup> M. G. Henderson,<sup>4</sup> and M. I. Sitnov<sup>5</sup>

Received 27 June 2013; revised 11 September 2013; accepted 13 September 2013; published 29 October 2013.

[1] As the Polar spacecraft apogee precessed through the magnetic equator in 2001, Polar encountered numerous substorm events in the region between geosynchronous orbit and 10  $R_E$  geocentric distance; most of them in the plasma sheet boundary layers. Of these, a small number was recorded near the neutral sheet in the evening sector. Polar/Thermal Ion Dynamics Experiment provides a unique perspective on the lowest-energy ion plasma, showing that these events exhibited a damped wavelike character, initiated by a burst of radially outward flow transverse to the local magnetic field at  $\sim 80$  km/s. They then exhibit strongly damped cycles of inward/outward flow with a period of several minutes. After one or two cycles, they culminated in a hot plasma electron and ion injection, quite similar to those observed at geosynchronous orbit. Cold plasmaspheric plasmas comprise the outward flow cycles, while the inward flow cycles contain counterstreaming field-parallel polar wind-like flows. The observed wavelike structure, preceding the arrival of an earthward moving substorm injection front, suggests an outward displacement driven by the inward motion at local times closer to midnight, that is, a “snowplow” effect. The damped in/out flows are consistent with interchange oscillations driven by the arrival at the observed local time by an injection originating at greater radius and local time.

**Citation:** Moore, T. E., M. O. Chandler, N. Buzulukova, G. A. Collinson, E. L. Kepko, K. S. Garcia-Sage, M. G. Henderson, and M. I. Sitnov (2013), “Snowplow” injection front effects, *J. Geophys. Res. Space Physics*, 118, 6478–6488, doi:10.1002/jgra.50573.

### 1. Introduction

[2] The night sector of the inner plasma sheet is characterized by highly dynamic behaviors as part of the phenomenology of substorms [Reeves *et al.*, 1996]. That which had been referred to as a “substorm injection boundary” [McIlwain, 1974] came to be seen by multiple spacecraft as the result of a “propagating injection front” [Moore *et al.*, 1981], which also propagates azimuthally [Arnoldy and Moore, 1983]. This could be attributed to an earthward “convection surge” [Quinn and Southwood, 1982; Mauk, 1986]. This interpretation was challenged by Lopez and Lui [1990], who suggested a near-Earth initiation followed by tailward propagation based on magnetic field and energetic particle observations. The convection surge phenomenology came to be described

as “bursty bulk flows” by Angelopoulos *et al.*, 1994, who showed statistically that such disturbances are azimuthally localized, but radially extended events, consisting of prominent channels of strong and dynamic flow. MHD models of “bubbles” were developed [Chen and Wolf, 1999] that exhibit a similar phenomenology. When lobe reconnection occurs, it creates newly closed but stretched flux tubes with insufficient plasma content to support the freshly reconnected magnetic flux tube. These contract vigorously toward Earth, becoming more dipolar as they contract or “dipolarize”. Kinetic modeling of the dipolarization-injection process showed substantial single-particle energy and plasma pressure gains [Delcourt and Sauvaud, 1994; Fok *et al.*, 1999].

[3] Despite additional indications of earthward motion near geosynchronous orbit, there has been considerable doubt and confusion about where the substorm disturbance originates, how it propagates, and what its place is in the overall substorm morphology. Cluster observations [Nakamura *et al.*, 2002; Takada *et al.*, 2006] again emphasized the earthward propagation of dipolarization fronts or even entire plasmoids [Zong *et al.*, 2004]. But the multispacecraft Time History of Events and Macroscale Interactions during Substorms (THEMIS) mission brought focus to the radial evolution of substorm phenomena in this region [Angelopoulos *et al.*, 2008]. More recently, THEMIS has conclusively shown [Runov *et al.*, 2009, 2011; Lee *et al.*, 2012] that a “dipolarization front” originates with a gust of earthward-directed flow generated by magnetotail reconnection, and propagates radially earthward, for a substantial fraction of substorm events. More recently,

<sup>1</sup>NASA’s Goddard Space Flight Center, Code 670, Greenbelt, Maryland, USA.

<sup>2</sup>NASA’s Marshall Space Flight Center, EV44, Huntsville, Alabama, USA.

<sup>3</sup>Department of Astronomy, University of Maryland, College Park, Maryland, USA.

<sup>4</sup>Los Alamos National Laboratories, MS-D466, Los Alamos, New Mexico, USA.

<sup>5</sup>Johns Hopkins University Applied Physics Laboratory, Laurel, Maryland, USA.

Corresponding author: T. E. Moore, NASA’s Goddard Space Flight Center, Code 670, Greenbelt, MD 20771, USA. (thomas.e.moore@nasa.gov)

simulations have begun to describe the dipolarization front process [Sitnov and Swisdak, 2011] and the kinetic structure of the dipolarization front has become a topic of great interest [e.g., Sergeev et al., 2009].

[4] The midterm phase of the Polar mission fortuitously placed the spacecraft apogee near the equatorial plane as it swung through the magnetotail in 2001–2002. During this phase, many substorm dipolarization events were observed, at times with multiple occurrences during a single pass through the plasma sheet at geocentric distances up to 9.5  $R_E$ . Generally, such events appear as fast rotations of the local magnetic field from highly stretched in the  $X_{GSM}$  direction, to more dipolar in orientation. During such rotations, the outflowing polar wind streams that fill the lobes adjacent to the plasma sheet, that is, the Lobal winds of Liemohn et al. [2005], flow strongly transverse to the local magnetic field, corresponding to the earthward relaxation of stretched flux tubes. Polar was equipped with a sensitive low-energy plasma instrument capable of observing such lobal wind flows and offers a unique perspective on the behavior of plasma and fields in this region. While such low-energy plasmas are often hidden by adverse spacecraft potentials [André and Cully, 2012], they become visible when high flow velocities, such as those in substorm flows, raise their energy relative to Polar.

## 2. Context

[5] The Polar mission has been described extensively elsewhere [Russell, 1995]. For present purposes, its principal assets were an unusually capable low-energy plasma instrument [Moore et al., 1995], the hot plasma instrument [Russell, 1995], and the magnetometer [Russell, 1995]. The focus here will be on events with time scale of 5–10 min. Therefore, single spin resolution ( $\sim 6$  s) is adequate to resolve the features of interest.

[6] The quiescent plasma sheet as observed from the Polar orbit with apogee near the neutral sheet and at L values up to 10  $R_E$  comprises magnetic field  $X_{GSM}$  and  $Z_{GSM}$  components that vary gradually as the spacecraft travels from negative to positive magnetic latitude. The lobal wind regions [Liemohn et al., 2005] outside the plasma sheet proper are filled with low-density outflows containing a mixture of high Mach number light ion polar wind and dayside auroral outflows as also reported, with composition, by Kistler et al. [2010]. Embedded sporadically within these lobal wind flows, we find much hotter and lower Mach number flows from the nightside auroral zone. When the plasma sheet is activated by convection, the reversal of the field between the hemispheres thins into an ion-scale current sheet, containing a plasma sheet population of relatively isotropic electrons and ions surrounded by regions of counterstreaming low-energy ions presumably formed by the convection of anti-sunward streams from both lobes onto closed flux tubes, where they naturally interstream with each other [Liemohn et al., 2005].

[7] When the plasma sheet becomes not only active, but denser with plasmas, including denser supply flows of the lobal and auroral winds, the result is one or more discrete dipolarizations as illustrated in Figure 1. This pass features four distinct dipolarization events observed as the spacecraft progresses from negative to positive magnetic latitudes, with

one of the dipolarizations occurring near the neutral sheet crossing at about 13:50 UT. At several points in the figure, for example, just before 16:00 UT, and as illustrated by the inset velocity distribution, it can be seen that the cold plasma stream nominally aligned with the local magnetic field direction is substantially shifted off that direction by transverse inward flow comparable to the parallel flow. A fit to the ion flux peak yields a field-perpendicular motion of the plasma toward the neutral sheet of approximately 89 km/s, assuming protons, with a substantially smaller thermal speed corresponding to between 0.8–1.1 eV temperature, and a density of  $\sim 0.015$  /cm<sup>3</sup>. The pass in Figure 1 is believed to be reasonably typical and illustrative of the effect of individual dipolarizations on the low-energy lobal and auroral wind plasma at this location near the plasma sheet boundary layer [Liemohn et al., 2005]. Sampling of the cold plasma component at such low densities has not routinely been feasible in the past, but became sporadically possible using the Thermal Ion Dynamics Experiment (TIDE) instrument on Polar. Designed specifically for polar wind observations, it has a very large effective area exceeding 1 cm<sup>2</sup> for each of a fan of seven apertures, and a detectability threshold, depending on flow velocity, of well under 1 cm<sup>-3</sup>, as is clear from Figure 1.

[8] For comparison, Figure 1 (bottom) shows spectrograms of electrons and ions from the LANL geosynchronous spacecraft for the same period, in which multiple discrete injection signatures can readily be identified, corresponding to the dipolarizations and cold plasma flows identified at POLAR at its location. From this comparison it is evident that the inner plasma sheet was disturbed on this day by multiple successive substorms, with a repetition period of about 2 h, so this is an example of a “sawtooth” injection event.

[9] As the 2001 fall season progressed, Polar sampled regions progressively west of the main substorm dipolarization region near midnight, eventually encountering a different set of phenomena, though still associated with substorm dipolarization. Owing to the nature of the Polar Orbit, the number of events was insufficient to perform statistical studies, but we report the characteristics of two specific events below.

## 3. Observations

[10] We begin by illustrating the orbital segments from which the specific observations originate. Figure 2 shows that event 1 at 10:15 UT on 11 Nov 2001 occurred when Polar was at 9.5  $R_E$  geocentric distance, at a magnetic local time of 21.2°, and at magnetic latitudes near the equator, ranging from 1.5 to 2.5°. Event 2 at 09:20 UT on 20 Dec 2001 occurred when Polar was at 9.5  $R_E$  geocentric distance, at a magnetic local time of 18.5°, at a range of magnetic latitudes ranging from 4 to 5.5°. Thus, both events occurred in the early evening sector, well before local midnight, within a few degrees of the magnetic equator, and at a distance well outside geosynchronous orbit.

[11] For event 1 on 11 November (DOY 315), the average solar wind velocity was  $\sim 400$  km/s, with density  $\sim 2$  particles per cubic cm, with average field intensity of  $\sim 5$  nT. The solar wind had been quiet for the previous 4 days, with  $B_z \sim 0 \pm 4$  nT. For event 2 on 20 Dec (DOY 354), the average solar wind velocity was  $\sim 300$  km/s with density  $\sim 3$  particles

Event 0: 2001 Oct 22 (22:30 MLT)

15:59:36 UT  
 2-D Fit parameters:  
 Density:  $0.015 \text{ cm}^{-3}$   
 $V_{\text{para}}$ : -28.0 km/s  
 $V_{\text{perp}}$ : -89.0 km/s  
 $kT_{\text{para}}$ : 1.10 eV  
 $kT_{\text{perp}}$ : 0.80 eV

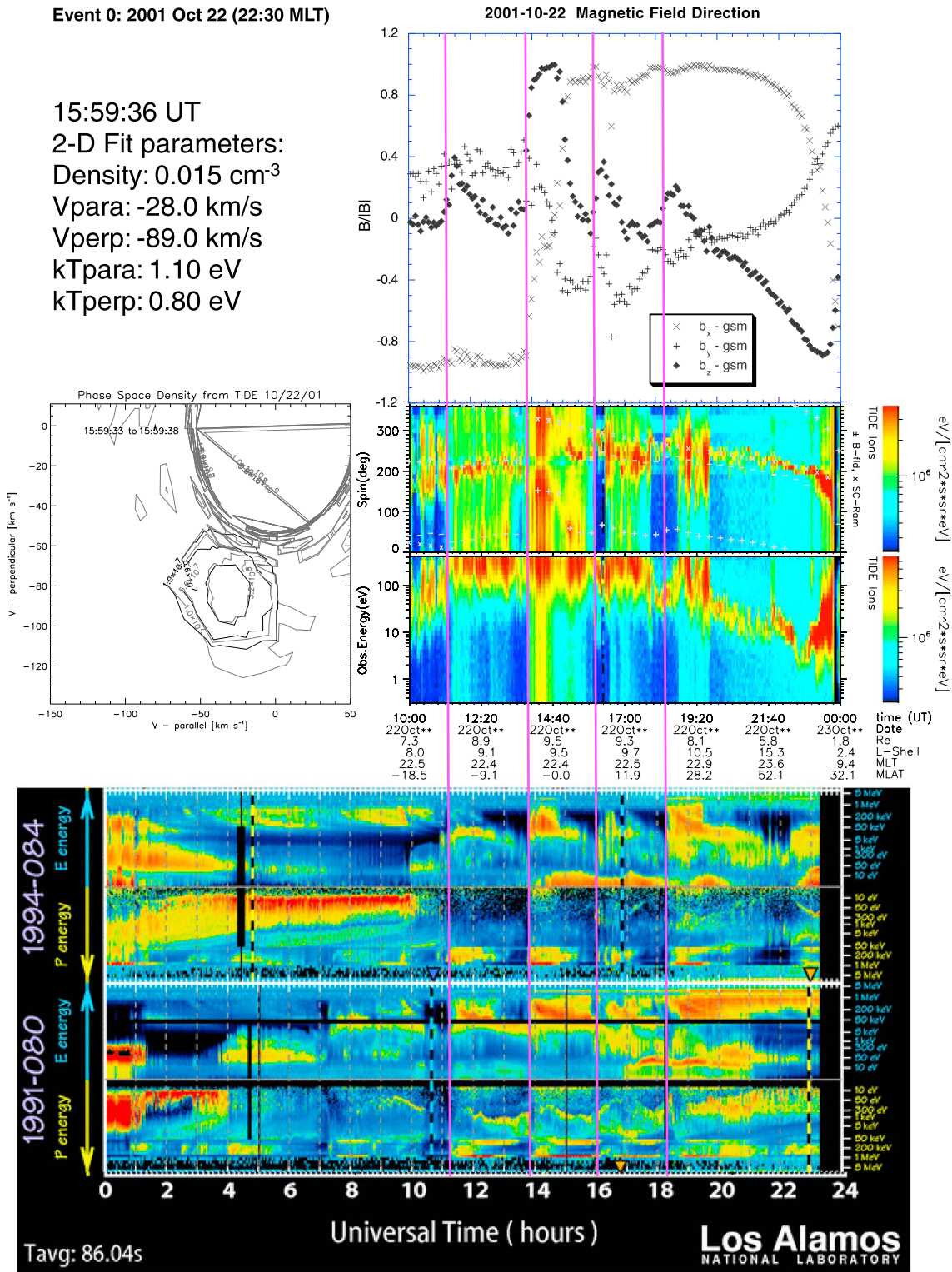
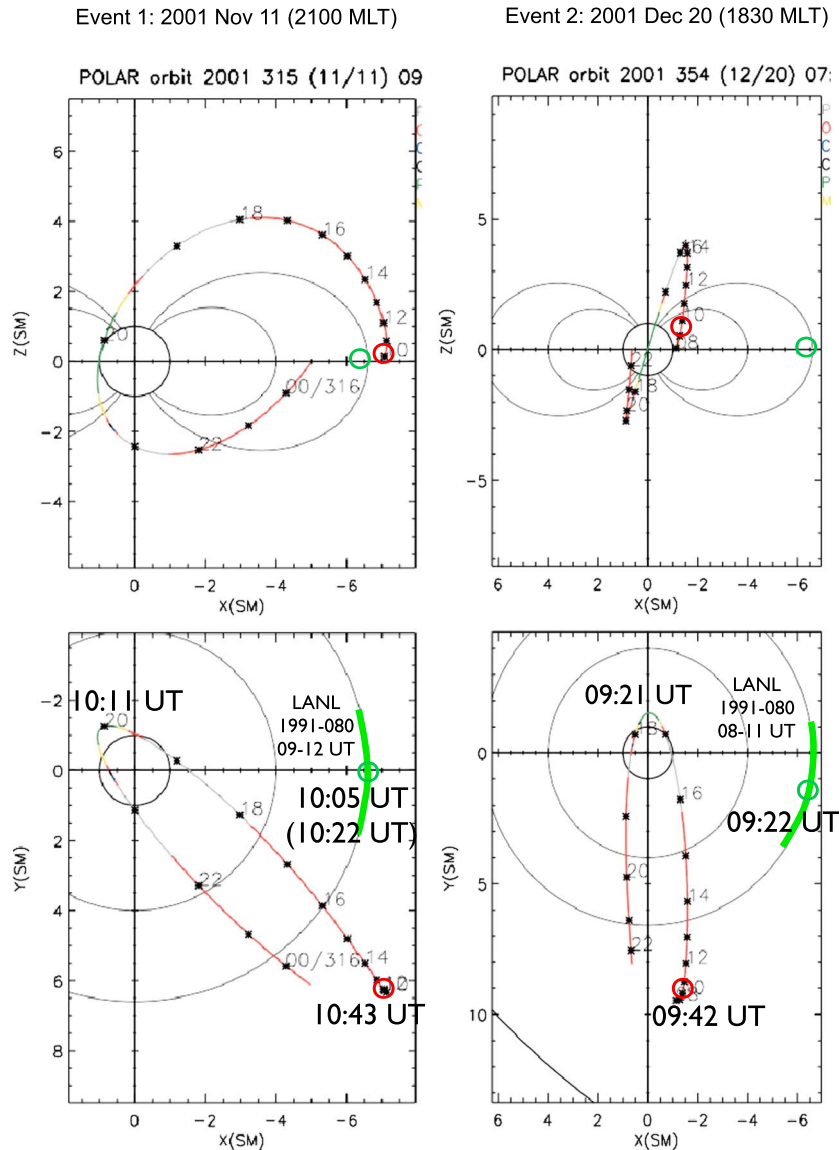


Figure 1. Observations from a Polar pass through the very active nightside plasma sheet during which multiple substorm dipolarizations were observed.

per cubic cm, also with average field strength of  $\sim 5$  nT, and the solar wind had been quiet for the previous 2 days with  $B_z \sim 0 \pm 5$  nT. The SuperMAG substorm database [Gjerloev, 2012] includes three substorm records for the day preceding event 1, and shows a single substorm on the day of event 1, with an onset at 10:23 UT. SuperMAG

reports five substorms on the day preceding event 2, but no recorded substorms on the day of event 2. These records suggest that the events 1 and 2 were isolated injection events associated with relatively quiet day activity, after typical activity without unusual forcing of the magnetosphere, leading up to these events.



**Figure 2.** Polar (red) and synchronous spacecraft (green) orbits for the events 1 and 2. Red curves/circles indicate Polar orbit/position at events 1 and 2 injections. Green curves/circles indicate LANL spacecraft orbits/positions during events 1 and 2, as indicated.

[12] In Figure 3 we characterize these two events using ground magnetic data, to be compared with the Polar magnetometer for reference. For event 1 on 11 Nov, there is a substorm beginning  $\sim 10:10$ – $10:11$  h, with a 10:35 intensification, with a clear Pi2 onset (not shown), observed at MMB (Memambetsu, Kakioka Magnetic Observatory). Event 1 produced negative bay activity at multiple Canopus stations, as shown.

[13] In addition, the IMAGE FUV auroral imaging team (H. U. Frey, private communication, 2013) reports a substorm for event 1 with onset time of 10:25:30 UT at 23.7 h MLT and 72.85° MLat. The POLAR UVI auroral imager had a poor view of the southern auroral oval for this event but reports a southern auroral enhancement at 10:24 UT, near 22 MLT. It was not clear from the UVI imagery that the enhancement was associated with a substorm (K. Liou, private communication, 2013).

[14] Event 2 on 20 Dec 2001, had a high-latitude negative bay, recorded at Dawson, of 200 nT  $x$  component beginning

at  $\sim 09:21$ – $09:22$  h. Event 2 was more localized and isolated than event 1 at the Earth's surface, and did not result in a substorm entry in the SuperMAG database. POLAR UVI reports (K. Liou, private communication) a short-lived brightening at 09:53 UT, at 19 MLT. Unfortunately, neither the POLAR nor the IMAGE auroral imagers were able to provide definitive auroral observations of this event owing to orbital positions near the equator and the high latitude of the events.

[15] The ground magnetometer view of these events is complemented by a view of geosynchronous plasma from the LANL spacecraft, as shown in Figure 4. Here spacecraft 1994–080 is in the evening sector during both events 1 and 2, and clearly sees both events as injection signatures, with dispersive electron flux increases, from low to high energy, in close association with the magnetic bay signatures from ground magnetometer data. At this spacecraft, event 1 has two separate dispersive increases from low- to high-energy

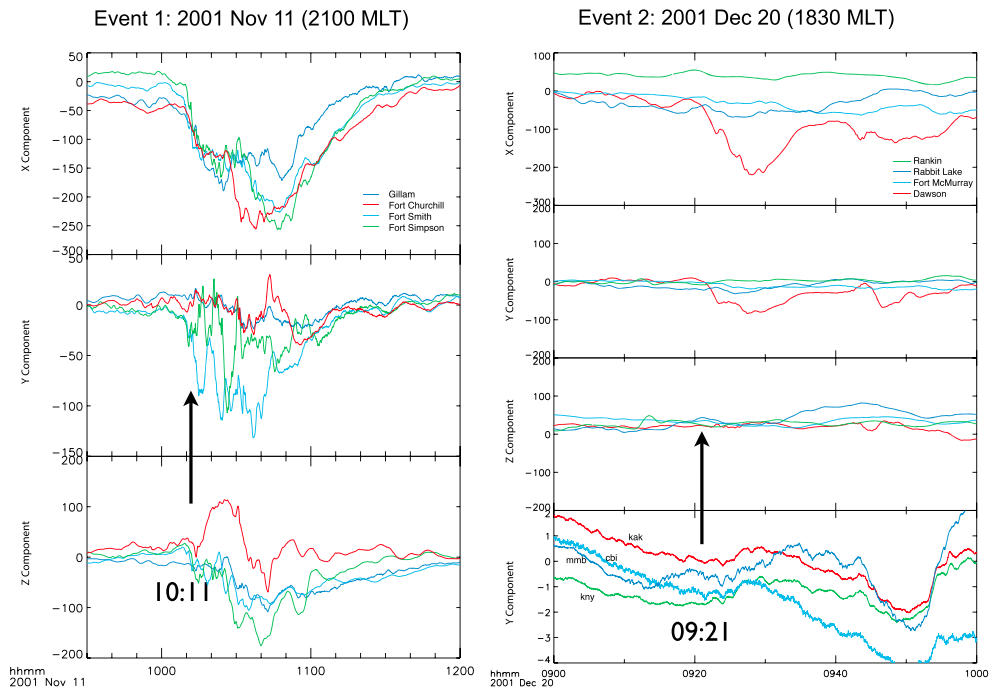


**Figure 3.** Event 1: X, Y, and Z components’ auroral zone magnetic field data showing the onset of a moderate substorm near 1010 UT. Event 2: X, Y, and Z components’ auroral zone magnetic field data showing the onset of a small, localized negative bay beginning ~0920 UT, and low-latitude, Y component magnetic field data from stations of the 210°MM array showing small Pi2 pulsations beginning near ~0920 UT.

electrons, presumably corresponding to structure in the ground signature. The earlier of the two precedes the ground onset by a few minutes; the latter succeeds it. For event 2, the negative bay signature begins only about a minute or two before the geosynchronous injection. Unfortunately, we could not locate a Pi2 signature in available ground magnetometer data for event 2, but it is evident from the geosynchronous observations that event 2 is a substorm.

[16] Also of great interest is that a prominent cold ion signature can be seen at the lowest ion energies, for hours leading up to both of these events, and ending with the hot plasma injections. Such cold plasma is observed to appear

at geosynchronous orbit in association with substorm growth phase [Moldwin *et al.*, 1996] and after periods of prolonged geomagnetic quiet [Sandel *et al.*, 2003].

[17] The main data for this study of the events is contained in Figure 5 where we have stacked Polar magnetometer data with Polar hot plasma electrons and ion energy spectrograms, and finally with the low-energy plasma energy and spin angle spectrograms. These data sets attest to the occurrence of substorm injections of hot electron plasmas at the Polar location for each event, as indicated. The injection is slightly dispersive in each case, with lower energy electrons arriving first. This is usually interpreted as the motion of a spatially

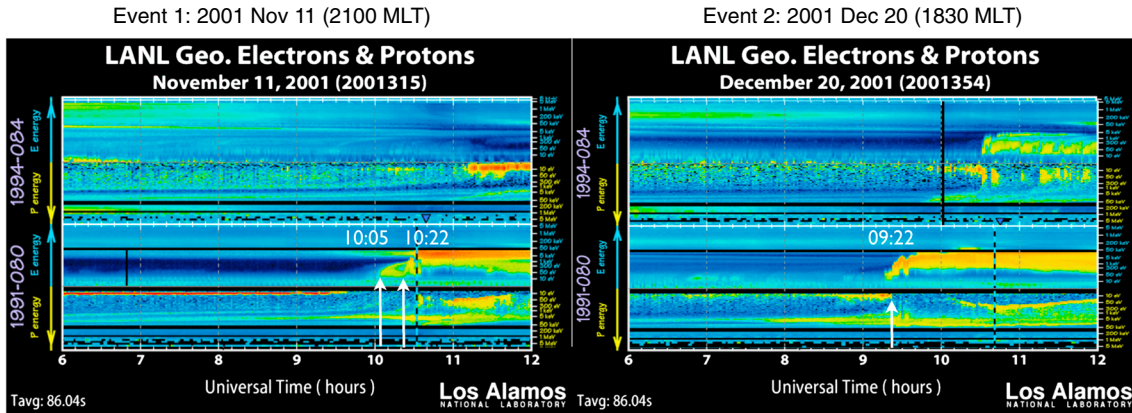


**Figure 4.** Geosynchronous overview of events 1 and 2 from the indicated LANL spacecraft. Midnight crossings are indicated by the dashed vertical lines. Events 1 and 2 injections at Polar are indicated by the white arrows with injection times indicated.

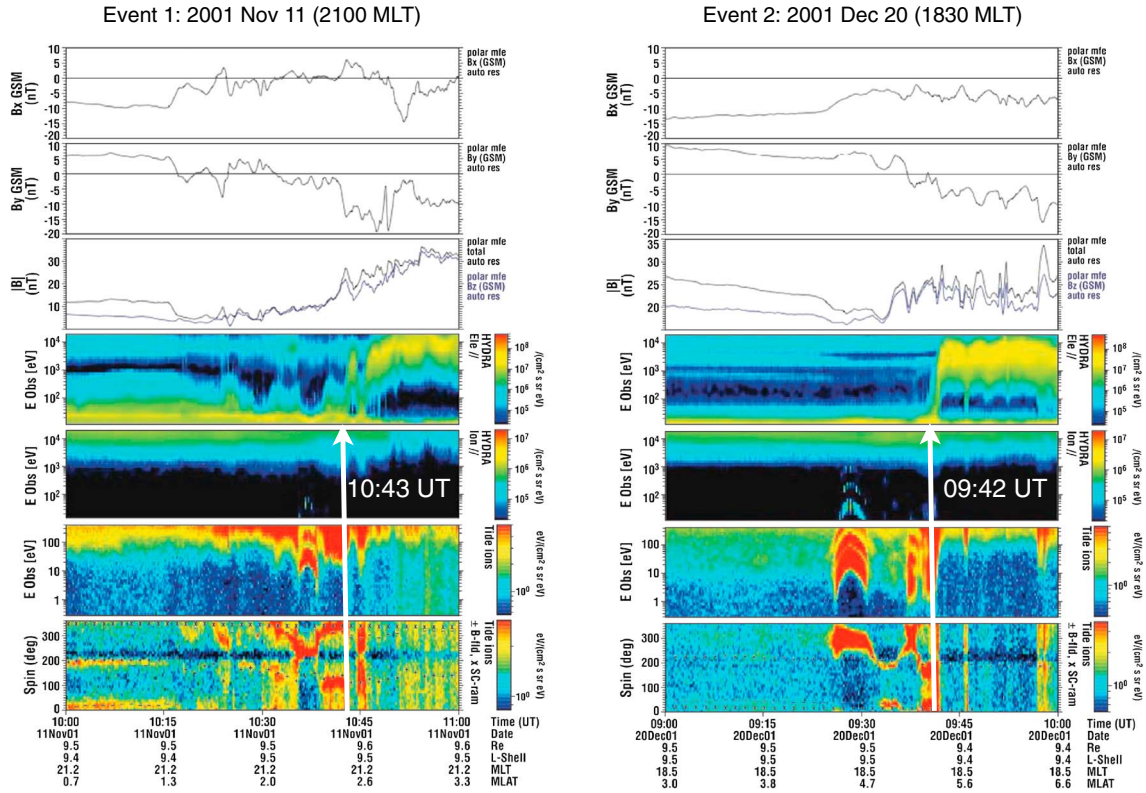


**Figure 5.** Stack spectrogram plots of events 1 and 2 data from the Polar spacecraft.

dispersed boundary over the spacecraft, consistent with the identification of these events as substorm injection fronts that can be modeled as convection surges [Moore *et al.*, 1981; Mauk, 1986].

[18] That the events involve field dipolarizations can be seen from the behavior of the  $B_z$  component and total magnitude of the Polar magnetic field, which shows a jump that is coincident with the electron plasma injection leading edge. The dipolarization is not quite classic in nature because that would imply a decrease in the magnitude of the  $B_x$  and  $B_y$  components. Still, the substantial ( $\sim 100\%$ ) increase in the magnitude of the local magnetic field at Polar is strongly indicative of a dipolarization with relaxation of field that was previously stretched beyond the Polar position. For event 1, there is a wavelike injection feature, rather than a step-like one. We interpret this as a corresponding wavelike motion of the boundary, and will return to this point in the discussion to follow.

[19] In the bottom panels of Figure 5, the low-energy ion plasma can be seen to be active in complex patterns for these events. Similar low-energy features can also be seen in the Hydra energy spectrograms, albeit with lower count rates. Along the lines also reported, for example, by Waite *et al.* [1986]; Chandler and Moore [2003], and Hirahara *et al.* [2004], we interpret the multiple traces in the energy spectrograms as the presence of multiple ion species in a cold plasma that is flowing rapidly transverse to the local magnetic field at the spacecraft. During this period, TIDE is not performing time of flight mass analysis, but its energy analysis is sufficient to separate species under conditions of common transverse convection, much as it is in the supersonic polar wind. It can also be seen in both events that the periods of

cold rapid flow are separated by periods of bidirectional streaming. In each case there are cycles of oscillation between cold supersonic flow and bidirectional streaming. When account is made of the spacecraft attitude in the interpretation of the angular distributions, it becomes evident that the observed transverse cold flow is radially away from the Earth, while the observed bidirectional streaming along the local magnetic field direction contains a component that is radially toward the Earth.

[20] This complex oscillatory flow structure is exhibited well in Figure 6, in which the low-energy ion data is interpreted as velocity distribution functions in the spin plane of the orbit normal spinning spacecraft, at snapshot times reflecting the extremes of the inward and outward motion with respect to the Earth. Here the projection of the local magnetic field into the spin plane is illustrated and the labels indicate tilt angle out of that plane. For the 11 Nov event (1), the spacecraft spin axis is oriented obliquely to GSM coordinates and the tilt of the local field is relatively large, so the projection of the velocity distributions to the GSM  $V_x$ - $V_z$  system results in obvious elliptical distortion of the distribution. For the 20 Dec event (2), which is near the dusk meridian, the same projection is relatively circular since the spin axis nearly coincides with the GSM  $x$  axis and the field tilt from the spin plane is smaller. For purposes of these plots, all ions are treated as  $H^+$  (protons), but it should be kept in mind that there is evidence of heavier ions as well.

[21] In both cases, it can be seen in Figure 6 (top row) that the distributions are well characterized as cold but rapid flows radially away from the Earth (positive  $V_y$  for 20 Dec, and negative  $V_x$  for 11 Nov). Secondary peaks correspond to minor ion species ( $He^+$  and  $O^+$ ). Conversely, it can be seen

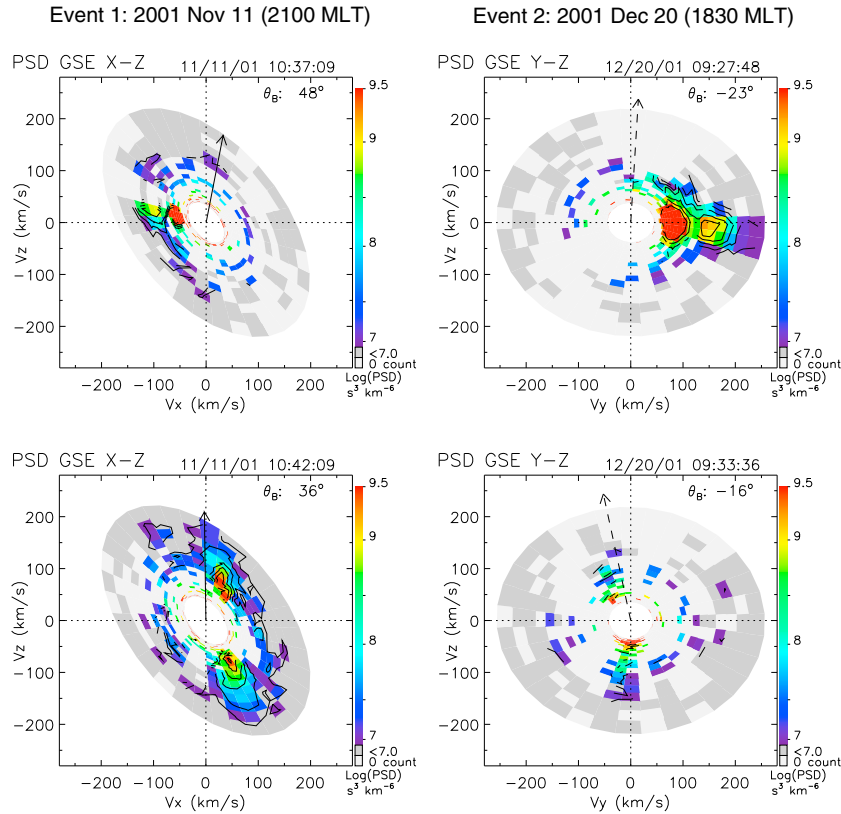


**Figure 6.** Polar/TIDE low-energy ion velocity distributions illustrating (top) outward motion, and (bottom) inward motion with parallel streaming. For event 1, the spin plane is projected onto the GSE X-Z plane, since the spacecraft is closer to midnight; while for event 2, it is projected onto GSE Y-Z plane since the spacecraft is closer to dusk. Arrows indicate the direction radially away from Earth in each panel.

in Figure 6 (bottom row) that the distributions are well described as cold counterstreaming field-aligned flows having an overall motion that is radially toward the Earth ( $-V_y$  for 20 Dec and  $+V_x$  for 11 Nov).

[22] As can be appreciated from Figure 6, the low-energy plasma, less than 300 eV, provides the best measure of the lower order moments of density and flow. For the hotter plasma observed by Hydra, these moments are uncertain owing to low counting statistics for the lowest-energy plasma, though of course inclusion of the hot plasma is essential to a computation of pressure or higher moments. The density correction produced by inclusion of the hot plasma is both uncertain and fractionally small compared with the cold plasma density.

[23] Values of flow velocity and estimates of thermal speeds can be read approximately from the plots in Figure 6. The radial outward flow speeds are  $\sim 80$  km/s, while the thermal speeds are somewhat smaller than that. The duration of these flows is on the order of 3 min or 180 s, leading to a rough estimate of the amplitude of the flow oscillations of  $1.5 R_E$  in both cases. In Figure 7, we display standard computed moments of the low-energy plasma for the two events described above, which firm up the estimates made from Figure 6. No effort is made to separately compute moments for the counterstreaming flows seen in Figure 6, so the counterstreaming appears as a parallel temperature enhancement. These moments are calculated after first correcting measured ion energy for the (generally positive)

spacecraft potential reported by the EFI experiment on Polar. This potential was reduced when low-energy density increased, and also when the flux of hot electrons observed by Hydra increased.

[24] Event 1, observed near 2100 MLT, begins with a period of sporadic flows of ions in the few 100 eV range, which are generally double peaked in pitch angle, and counterstreaming parallel to the magnetic field. Then, a radially outward (perpendicular to the local magnetic field) flow burst occurs, followed by a cycle of inward flow and then a weaker outward flow. During the first and strongest outward flow cycle, the core thermal energy drops below 10 eV. In the inward flow cycles, a distinct enhancement of the parallel temperature corresponds to the parallel counterstreaming that is clearly visible in both the spectrograms of Figure 5 and in the velocity distributions of Figure 6. This culminates in the hot electron appearance that is the signature of substorm injections in the equatorial middle-magnetosphere, very similar to that observed near midnight and some 20 min earlier, at geosynchronous orbit, as shown in Figure 4.

[25] Event 2, observed near 1830 MLT, begins with a pronounced radially outward (perpendicular to local magnetic field) flow burst, followed by an inward flow cycle, then a second outward cycle, and finally another inward cycle, culminating in the hot electron injection seen in Figure 5. During the first and strongest outward flow, the cold ion temperature falls below 10 eV and below 5 eV in the parallel direction. During the inward flow cycles, a

Event 1: 2001 Nov 11 (2100 MLT)

Event 2: 2001 Dec 20 (1830 MLT)

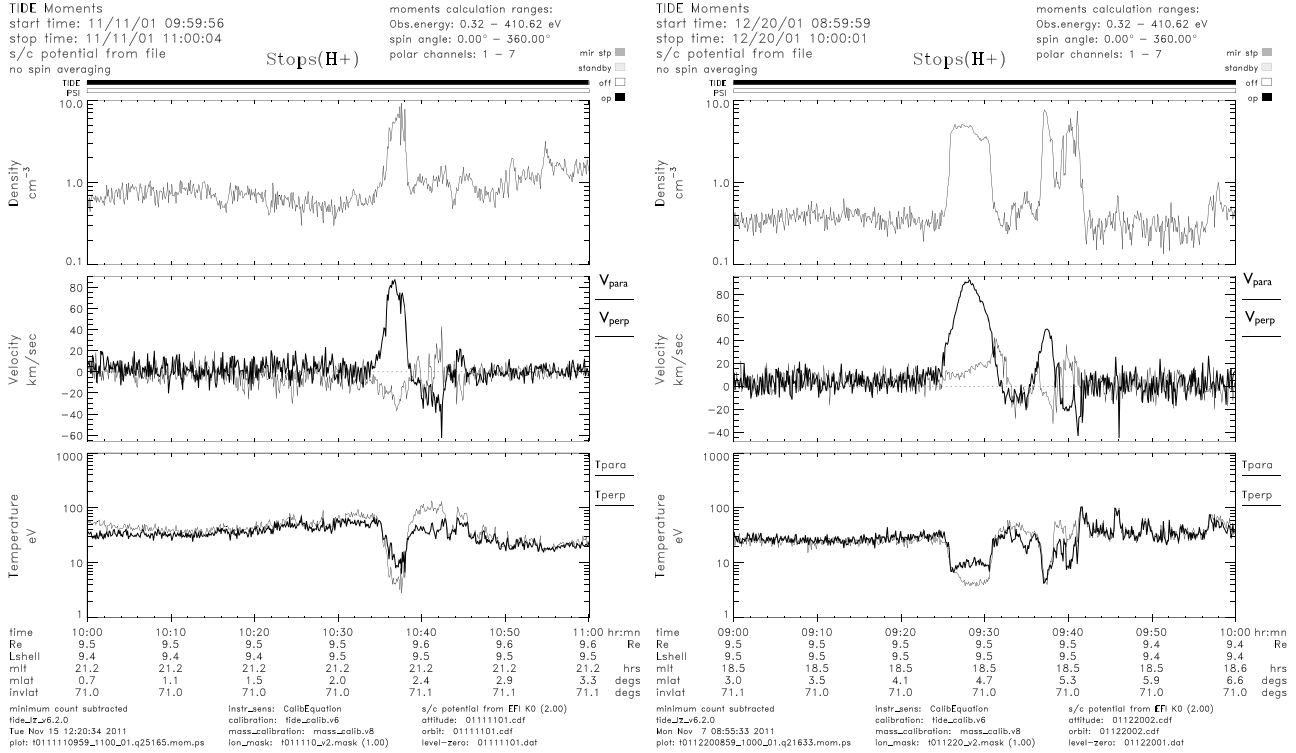


Figure 7. Polar/TIDE low-energy ion moments for events 1 and 2.

distinct enhancement of the parallel temperature corresponds again to the parallel counterstreaming so visible in the spectrograms and velocity distribution plots of Figure 6. An inward flow cycle culminates in the appearance of the hot electron injection that occurred some 20 min earlier at geosynchronous orbit, as shown in Figure 4.

[26] In both of the events 1 and 2, there also appear to be distinct oscillations in the parallel flow velocity. Keeping in mind that this flow velocity is a sum over two counterstreaming beams, it appears that the oscillation corresponds to a fluctuation in the flow or density of the individual streams, though we have not looked at this in detail here. The two events are strikingly similar, despite their wide separation in MLT. Generally, it may be said that event 1, the closer of the two to midnight, is dominated to a greater extent by the warm counterstreaming plasmas, while event 2, the more distant of the two from midnight, is more dominated by the cold outer plasmaspheric plasmas. However, both events exhibit the same general type of radial oscillations of the plasma flow and culminate in very similar substorm hot plasma injections, delayed relative to the same injections as seen at geosynchronous orbit and farther to the east.

[27] The relative timing of these events is summarized in Figure 2. As seen on the ground, at synchronous orbit, and at Polar, the relative timing demonstrates the westward propagation of an injection front that appears first in the midnight sector, and expands to the west at a rate of  $\sim 4$  h LT per 20 min, or 0.2 h LT per minute. *Arnoldy and Moore* [1983] reported on the basis of statistical study, that “the synchronous orbit manifestation of substorms, i.e., plasma injection and magnetic field reconfiguration to dipolar, has an onset

that expands both eastward and westward from a relatively narrow sector near midnight.” Moreover, they reported essentially the same rate of expansion that we find here. Thus, we interpret events 1 and 2 as the westward extent of substorm manifestations that were initiated in a narrow sector near midnight LT.

#### 4. Discussion

[28] The following briefly summarizes the salient facts revealed by the observations shown above:

[29] 1. In the evening to dusk sector of the magnetosphere, inward moving midnight sector injection-dipolarization events propagate west across the evening sector and are preceded by a transient outward flow with one or two damped cycles of flows and field variations in the ULF range (several minute periods), culminating in the decisive inward injection of hot plasma.

[30] 2. The observed oscillations occur at a boundary between very cold ( $< 10$  eV) ion plasmas resembling low-density outer plasmaspheric material and plasmas that include prominent field-aligned counterstreaming populations of cold ions characteristic of the polar-auroral-lobal wind. The hot plasma injection adds a hot (few keV) electron population (and tens of keV ions) characteristic of injections at the inner edge of the plasma sheet during substorm injections.

[31] 3. The amplitude of the outward cycle motion is  $\sim 1$  Re, so the thickness scale of the boundary between cold and counterstreaming plasmas is similarly of this order, or smaller.

[32] The 3-D structure of these features is ambiguous from single spacecraft or widely spaced measurements. It is

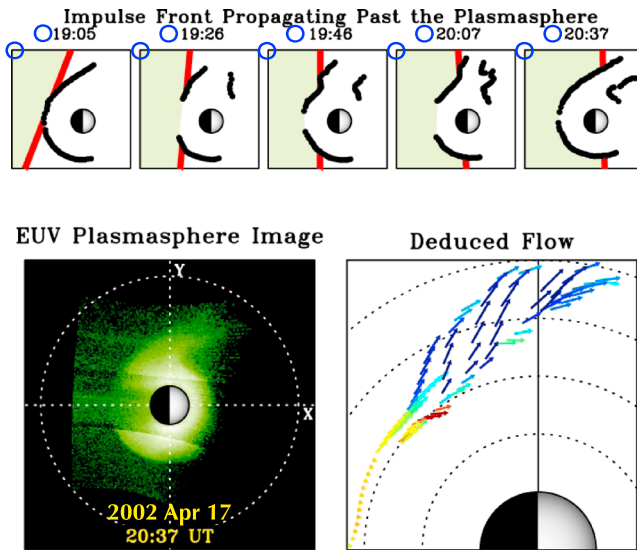


**Figure 8.** Schematic diagram of “snowplow” injection in EUV images by the IMAGE spacecraft for an injection event on 17 April 2002 [Goldstein *et al.*, 2005]. Blue circles schematically illustrate the relative position of Polar for events 1 and 2.

consistent with a “snowplow” wave in the plasma sheet inner boundary that is propagating westward past the Polar spacecraft as the substorm injection spreads westward from the midnight sector toward the dayside through the dusk sector. Such waves have been remotely imaged in EUV scattered from plasmaspheric  $\text{He}^+$  as they transit the plasmopause region at about half the geocentric distance of those reported here, or  $\sim 4\text{--}5 R_E$  [Goldstein *et al.*, 2005]. The concept of a “snowplow wave” is schematically illustrated in Figure 8, reproduced courtesy of Jerry Goldstein from his study of an event of 17 April 2002. Unfortunately, similar imagery was not available for the events reported here. Moreover, with a threshold for detectability of  $\sim 30 \text{ cm}^{-3}$ , the EUV observations cannot be expected to successfully image regions with plasma densities in the range  $0.1\text{--}10 \text{ cm}^{-3}$  as reported here in Figure 7. Interestingly, the plasmaspheric ripple was seen only on the dusk side and not on the dawn side of the plasmasphere, which may point toward an amplitude variation along the schematically drawn straight black front shown in Figure 8.

[33] Buzulukova *et al.* [2008] modeled the plasmaspheric ripple described by Goldstein *et al.* [2005]. They were able to reproduce the ripple characteristics, and a wavy motion of the plasmasphere. They concluded that the ripple was formed as a result of interaction between plasmasphere and substorm injection. In this interpretation, newly injected plasma near midnight drifted to the dusk sector together with field-aligned currents near the edge of the injection, and produced the wavy structures in the ionospheric potential. In the extreme case of very strong localized injections, the system developed a pattern similar to the interchange instability in the inner magnetosphere [e.g., Sazykin *et al.*, 2002] with a number of ripples propagating along the boundary between cold plasmaspheric plasma and hot ring current plasma. The model used by Buzulukova *et al.* [2008] was different from MHD models of bubbles because it has external, imposed

magnetic field, and the limitations of bounce-averaging. However, the results qualitatively agree with the picture obtained for POLAR events where hot injected plasma interacts with the plasmasphere, causing wavy motion of plasma near the boundary of interaction.

[34] It seems clear that a wave front with a large radius of curvature passed through the outer plasmasphere, producing a propagating ripple in the plasmaspheric trough density gradient. Ahead of the front, the plasmasphere is being displaced radially outward, while behind the front it is displaced radially inward. Presumably, the outward displacement is a reaction to the advancing compression of the plasmasphere behind the front, propagating at a fast mode speed ahead of the front. A single oscillation from outward to inward flow would be similar to the behavior that we are reporting here, apart from the evidence of damped oscillation.

[35] Recently, inspired by careful THEMIS observations of oscillatory flows associated with bursty bulk flows [Panov *et al.*, 2010], Wolf *et al.* [2012] have interpreted these as interchange oscillations driven by the impact of low-entropy bubbles on the inner magnetosphere. This may be the origin of the oscillatory motion reported here. Indeed, the period of such oscillations obtained from the Wolf *et al.* [2012, equation (33)] agrees well with the observed period, when the density of the plasma is as high as  $10 \text{ cm}^{-3}$  of protons, as we observed in the outward flow cycles.

[36] An injection/dipolarization front originating in the magnetotail, and moving Earthward toward an arrival at the plasmopause region, must pass through the region in which Polar resides during the observations reported here. While the plasmopause often appears well-defined and localized at  $4\text{--}5 R_E$  in the IMAGE/EUV imagery, those same observations show that the plasmasphere is actually an extended structure with a density gradient that stretches all the way to the magnetopause on the dayside [Chandler and Moore, 2003; Foster *et al.*, 2004]. The extent of the plasmasphere in the dusk sector is known to depend on the prior history of geomagnetic activity, with greater extent the lower the level of such activity has been in the preceding hours and days. In this regard it is important to note that cold plasma was visibly present prior to these injection events, at geosynchronous orbit in the LANL spacecraft observations of Figure 4. This plasma is visible in spite of solar photoelectron emission from those spacecraft, owing to the electrical configuration of the solar arrays.

[37] It is also possible that the oscillation reported here could result from a vortex on the flank of the Earthward bulk flow channel corresponding to the driver of the dipolarization front. If one or more vortices like that moved azimuthally toward the dusk sector, the observed flow oscillations could perhaps be produced. Clearly, however, these must be regarded as boundary features such that the final result of the injection is to place the spacecraft enduringly on the hot plasma side of the dipolarization front.

[38] The data presented here clearly indicate the presence of low densities of cold plasma amounting to several cubic centimeters at the Polar spacecraft location, prior to the event and the resultant earthward displacement by the dipolarization/injection front. The timing of these events is consistent with the ground signature and LANL geosynchronous observations of the events, allowing for their known azimuthal propagation. The cold plasma population

is seen as a transient during these events, and is consistent with the very low density plasmaspheric trough beyond the plasmasphere, which may consist of interpenetrating polar wind streams that are relaxing to thermal distributions in the region explored here.

## 5. Conclusions

[39] We reported two clear observations of substorm injections at the Polar spacecraft when it was at apogee near the magnetic equator in the dusk to evening sector of the magnetosphere. In contrast with other observations, some distance away from the neutral sheet, these substorm injection events closely resembled those reported for these events at geosynchronous orbit, where spacecraft are more routinely near the magnetic equator or neutral sheet. That is, an impulsive magnetic change from stretched to more dipolar (by definition, a dipolarization) was accompanied by an abrupt appearance of keV electrons and tens of keV ions.

[40] These events were observed with an exceptionally capable low-energy plasma analyzer, the Thermal Ion Dynamics Experiment, which provides differential angular and energy distributions over the full sky and the range from 0.3 eV to 300 eV. Thus, we are able to resolve the cold plasma response, which is most sensitive to low velocity motions, and therefore provides a new view of such events. We were thus able to measure the detailed properties of the plasmasphere at  $10 R_E$  where densities range from  $1\text{--}10\text{ cm}^{-3}$ . We found that this outer trough part of the plasmasphere responds to the substorm dipolarization front as if it were a “snowplow,” and in a way that is strongly analogous to the response of the plasmopause proper at  $4\text{--}5 R_E$  to dipolarization fronts. However, instead of simply translating a smooth gradient in density at relatively constant temperature, we found these effects to occur at a steep gradient of the thermodynamic properties of the low-energy plasma. Inward of the boundary lies a nearly thermal, dense plasma; while outside the boundary lies a distinctly different plasma of lower density, consisting of counterstreaming cold flows of polar or lobal wind plasmas that have not had sufficient time to thermalize. In advance of injection-dipolarization front passage through this boundary, it expands outward in response to the approaching “snowplow,” then oscillates briefly in a damped motion before moving decisively earthward, placing the spacecraft in a much hotter plasma environment similar to that which was injected by the same substorms at geosynchronous orbit, a few  $R_E$  earthward, a few hours later in LT, and tens of minutes earlier than the injections reached Polar.

[41] **Acknowledgments.** The authors acknowledge support from the Polar-Wind-Geotail (Global Geospace) Program, the Goddard Heliophysics Science Division, the Magnetospheric Multiscale Mission Project, and other sources. For the ground magnetometer data, we gratefully acknowledge the following: CARISMA, Ian Mann; CANMOS; The S-RAMP Database, K. Yumoto, and K. Shiokawa; SuperMAG, Jesper W. Gjerloev.

[42] Robert Lysak thanks the reviewers for their assistance in evaluating this paper.

## References

André, M., and C. M. Cully (2012), Low-energy ions: A previously hidden solar system particle population, *Geophys. Res. Lett.*, *39*, L03101, doi:10.1029/2011GL050242.

Angelopoulos, V., C. F. Kennel, F. V. Coroniti, R. Pellat, M. G. Kivelson, R. J. Walker, C. T. Russell, W. Baumjohann, W. C. Feldman, and J. T. Gosling (1994), Statistical characteristics of bursty bulk flow events, *J. Geophys. Res.*, *99*(A11), 21,257–21,280, doi:10.1029/94JA01263.

Angelopoulos, V., et al. (2008), Tail reconnection triggering substorm onset, *Science*, *321*(5891), 931–935, doi:10.1126/science.1160495.

Arnoldy, R. L., and T. E. Moore (1983), Longitudinal structure of substorm injections at geosynchronous orbit, *J. Geophys. Res.*, *88*, 6123–6220.

Buzulukova, N., M.-C. Fok, T. E. Moore, and D. M. Ober (2008), Generation of plasmaspheric undulations, *Geophys. Res. Lett.*, *35*, L13105, doi:10.1029/2008GL034164.

Chandler, M. O., and T. E. Moore (2003), Observations of the geopause at the equatorial magnetopause: Density and temperature, *Geophys. Res. Lett.*, *30*(16), 1869, doi:10.1029/2003GL017611.

Chen, C. X., and R. A. Wolf (1999), Theory of thin-filament motion in Earth’s magnetotail and its application to bursty bulk flows, *J. Geophys. Res.*, *104*(A7), 14,613–14,626.

Delcourt, D. C., and J. A. Sauvaud (1994), Plasma sheet Ion energization during dipolarization events, *J. Geophys. Res.*, *99*(A1), 97–108, doi:10.1029/93JA01895.

Fok, M.-C., T. E. Moore, and D. C. Delcourt (1999), Modeling of inner plasma sheet and ring current during substorms, *J. Geophys. Res.*, *104*(A7), 14,557–14,569.

Foster, J. C., A. J. Coster, P. J. Erickson, F. J. Rich, and B. R. Sandel (2004), Stormtime observations of the flux of plasmaspheric ions to the dayside cusp/magnetopause, *Geophys. Res. Lett.*, *31*, L08809, doi:10.1029/2004GL020082.

Gjerloev, J. W. (2012), The SuperMAG data processing technique, *J. Geophys. Res.*, *117*, A09213, doi:10.1029/2012JA017683.

Goldstein, J., J. L. Burch, B. R. Sandel, S. B. Mende, P. C. Sonnerup, and M. R. Hairston (2005), Coupled response of the inner magnetosphere and ionosphere on 17 April 2002, *J. Geophys. Res.*, *110*, A03205, doi:10.1029/2004JA010712.

Hirahara, M., K. Seki, Y. Saito, and T. Mukai (2004), Periodic emergence of multicomposition cold ions modulated by geomagnetic field line oscillations in the near-Earth magnetosphere, *J. Geophys. Res.*, *109*, A03211, doi:10.1029/2003JA010141.

Kistler, L. M., C. G. Mouikis, B. Klecker, and I. Dandouras (2010), Cusp as a source for oxygen in the plasma sheet during geomagnetic storms, *J. Geophys. Res.*, *115*, A03209, doi:10.1029/2009JA014838.

Lee, D.-Y., H.-S. Kim, S. Ohtani, and M. Y. Park (2012), Statistical characteristics of plasma flows associated with magnetic dipolarizations in the near-tail region of  $r < 12 R_E$ , *J. Geophys. Res.*, *117*, A01207, doi:10.1029/2011JA017246.

Liemohn, M. W., T. E. Moore, P. D. Craven, W. Maddox, A. F. Nagy, and J. U. Kozyra (2005), Occurrence statistics of cold, streaming ions in the near-Earth magnetotail: Survey of Polar-TIDE observations, *J. Geophys. Res.*, *110*, A07211, doi:10.1029/2004JA010801.

Lopez, R. E., and A. T. Y. Lui (1990), A multisatellite case study of the expansion of a substorm current wedge in the near-Earth magnetotail, *J. Geophys. Res.*, *95*(A6), 8009–8017.

Mauk, B. H. (1986), Quantitative modeling of the “convection surge” mechanism of ion acceleration, *J. Geophys. Res.*, *91*(A12), 13,423–13,431, doi:10.1029/JA091iA12p13423.

McIlwain, C. E. (1974), Substorm injection boundaries, in *Magnetospheric Physics*, edited by B. M. McCormac, Reidel, Hingham, Mass.

Moldwin, M. B., M. F. Thomsen, S. J. Bame, D. J. McComas, and L. A. Weiss (1996), The appearance of plasmaspheric plasma in the outer magnetosphere in association with substorm growth, *Geophys. Res. Lett.*, *23*, 801–804.

Moore, T. E., R. L. Arnoldy, J. Feynman, and D. A. Hardy (1981), Propagating substorm injection fronts, *J. Geophys. Res.*, *86*(A8), 6713–6726, doi:10.1029/JA086iA08p06713.

Moore, T. E., et al. (1995), The thermal ion dynamics experiment and plasma source instrument, *Space Sci. Rev.*, *71*(1–4), 409–458, doi:10.1007/BF00751337.

Nakamura, R., et al. (2002), Motion of the dipolarization front during a flow burst event observed by Cluster, *Geophys. Res. Lett.*, *29*(20), 1942, doi:10.1029/2002GL015763.

Panov, E. V., et al. (2010), Multiple overshoot and rebound of a bursty bulk flow, *Geophys. Res. Lett.*, *37*, L08103, doi:10.1029/2009GL041971.

Quinn, J. M., and D. J. Southwood (1982), Observations of parallel ion energization in the equatorial region, *J. Geophys. Res.*, *87*(A12), 10,536–10,540, doi:10.1029/JA087iA12p10536.

Reeves, G. D., M. G. Henderson, P. S. McLachlan, R. D. Belian, R. H. W. Friedel, and A. Korth (1996), Radial propagation of substorm injections, International Conference on Substorms, in *Proceedings of the 3rd International Conference on Substorms*, edited by E. J. Rolfe and B. Kaldeich, Eur. Space Agency Spec. Publ., ESA SP-389, 579 pp., Versailles, Paris, France, 12–17 May.

Runov, A., V. Angelopoulos, M. I. Sitnov, V. A. Sergeev, J. Bonnell, J. P. McFadden, D. Larson, K.-H. Glassmeier, and U. Auster (2009), THEMIS observations of an earthward propagating dipolarization front, *Geophys. Res. Lett.*, *36*, L14106, doi:10.1029/2009GL038980.

- Runov, A., V. Angelopoulos, X.-Z. Zhou, X.-J. Zhang, S. Li, F. Plaschke, and J. Bonnell (2011), A THEMIS multicasestudy of dipolarization fronts in the magnetotail plasma sheet, *J. Geophys. Res.*, *116*, A05216, doi:10.1029/2010JA016316.
- Russell, C. T. (Ed) (1995), The global geospace program, *Space Sci. Revs.*, *71*, 1–4.
- Sandel, B. R., J. Goldstein, D. L. Gallagher, and M. Spasojevic (2003), Extreme ultraviolet imager observations of the structure and dynamics of the plasmasphere, *Space Sci. Rev.*, *109*, 25–46.
- Sazykin, S., R. A. Wolf, R. W. Spiro, T. I. Gombosi, D. L. De Zeeuw, and M. F. Thomsen (2002), Interchange instability in the inner magnetosphere associated with geosynchronous particle flux decreases, *Geophys. Res. Lett.*, *29*(10), 1448, doi:10.1029/2001GL014416.
- Sergeev, V., V. Angelopoulos, S. Apatenkov, J. Bonnell, R. Ergun, R. Nakamura, J. McFadden, D. Larson, and A. Runov (2009), Kinetic structure of the sharp injection/dipolarization front in the flow-braking region, *Geophys. Res. Lett.*, *36*, L21105, doi:10.1029/2009GL040658.
- Sitnov, M. I., and M. Swisdak (2011), Onset of collisionless magnetic reconnection in two-dimensional current sheets and formation of dipolarization fronts, *J. Geophys. Res.*, *116*, A12216, doi:10.1029/2011JA016920.
- Takada, T., R. Nakamura, W. Baumjohann, Y. Asano, M. Volwerk, T. L. Zhang, B. Klecker, H. Réme, E. A. Lucek, and C. Carr. (2006), Do BBFs contribute to inner magnetosphere dipolarizations: Concurrent cluster and double star observations, *Geophys. Res. Lett.*, *33*, L21109, doi:10.1029/2006GL027440.
- Waite, J. H., D. L. Gallagher, M. O. Chandler, R. C. Olson, R. H. Comfort, J. F. E. Johnson, C. R. Chappell, W. K. Peterson, D. Weimer, and S. D. Shawhan (1986), Plasma and field observations of a Pc5 wave event, *J. Geophys. Res.*, *91*(A10), 11,147–11,161.
- Wolf, R. A., C. X. Chen, and F. R. Toffoletto, (2012), Thin filament simulations for Earth’s plasma sheet: Interchange oscillations, *J. Geophys. Res.*, *117*, A02215, doi:10.1029/2011JA016971.
- Zong, Q.-G., et al. (2004), Cluster observations of earthward flowing plasmoid in the tail, *Geophys. Res. Lett.*, *31*, L18803, doi:10.1029/2004GL020692.